2

JHKL′M and 1.3-mm Observations of a Selection of Wolf-Rayet Stars

D.Y.A Setia Gunawan, P.M. Williams and K.A. van der Hucht

RESULTS of *JHKL′M* photometry and 230-GHz (1.3-mm) observations of a selection of 14 Wolf-Rayet stars are presented. The 230-GHz data were obtained using the SEST telescope, while the infrared data were from many observations with various telescopes at ESO, UKIRT, CST and AAT. Combined with MSX, IRAS and radio data from literature, we construct multi-epoch, multi-frequency energy distributions of these stars.
The flux-density distributions can be expressed as $S_\nu \propto \nu^\alpha$, with an averaged spectral index of $< \alpha >= 1.08$ (1σ=0.27). We observe that some stars show a change of trend in their energy distributions between the near-infrared data and the long-wavelength data.

2.1 Introduction

Wolf-Rayet (WR) stars are hot stars, with temperatures ranging from around 20 000 K up to 95 000 K. Therefore, the radiated energy peaks at ultraviolet wavelengths and falls off steeply toward long wavelengths. This makes them very faint sources at the infrared and radio region. However, some WR stars are known to form dust. The strong ultraviolet radiation can be absorbed by the dust and re-radiated brightly at infrared (IR) wavelengths. The dust emission is characterized by a Planckian spectrum, appearing like a hump in the (near) infrared, on top of the stellar continuum (e.g., Williams 1996).

WR stars are also known for their strong stellar winds with high velocities, responsible for their expanding atmospheres. The wind velocity is low at the base of the wind and grows faster as it goes further out, where it asymptotically reaches the terminal velocity. The dense wind emits free-free radiation, which at millimetre to radio wavelengths is expected to arise from the region where the velocity has reached a constant terminal velocity. At long wavelengths, a uniform ionized wind, moving at a constant velocity and with density falling off as the inverse square of the distance from the star, can be characterized by a power-law spectrum of

$S_\nu \propto \nu^{0.6}$ (Wright & Barlow 1975, Panagia & Felli 1975), where S is flux density and ν is frequency. This is an intermediate between the spectral index expected for free-free emission from optically thick plasma: $S_\nu \propto \nu^2$, and that from optically thin plasma: $S_\nu \propto \nu^{-0.1}$ (e.g., Williams 1996).

However, Williams (1999) noted that radio and millimetre observations show that the spectral indices are found to be around $\alpha \approx 0.7$ (where $S_\nu \propto \nu^\alpha$), which is slightly steeper than the model value above. The spectral index difference is suggested to be due to ionization gradients or deviations from an inverse-square density law (Williams 1999).

The spectral indices get even steeper as one observes at shorter wavelengths. Morris et al. (1993) examined the continuum energy distributions of WR stars over the wavelength range $\sim$0.1–1.0 micron, i.e., from the ultraviolet to near-infrared (NIR) wavelengths. They found that for wavelengths longer than $\sim$0.14 micron, the intrinsic continua may be represented by a power law with a single spectral index α. The distribution of the spectral indices has a Gaussian distribution with a mean of $\alpha = 0.85$ where $1\sigma = 0.4$. However, they did not see any correlation between α and spectral subtype in their large sample which comprises 129 Galactic, LMC and SMC WR stars.

Some WR stars are also observed to have radio flux densities which are much higher than the value expected from the thermal, wind emission, and referred to as non-thermal emitters. This bright radio emission is thought to originate in the region where the winds of the two massive stars collided (Usov 1992).

In this study we seek to find trends or differences in the long wavelength (NIR-millimetre-radio) energy distributions of WR stars: between single stars and binaries, between those with and without non-thermal emission. For this reason, we compile data from our observations in the IR (*JHKL′M* photometry), and in the sub-millimetre (sub-mm) region (230 GHz continuum) of a selection of WR stars. The spectral types, optical magnitudes and extinctions towards the stars in this study are shown in Tab. 2.1. We combine these IR and sub-mm data with available mid-IR data, i.e. from MSX (Midcourse Space eXperiment) satellite (Egan et al. 1999), and IRAS Point Source Catalogue (PSC), and various radio data. The observations are described in Sect. 2.2, the analysis and discussions in Sect. 2.2.3 and Sect. 2.3, and the results are summarized in Sect. 2.4.

2.2 Data and analysis

2.2.1 1.3-mm observations

We observed a sample of 22 Wolf-Rayet stars with the 15-m Swedish-ESO Sub-mm Telescope (SEST) at ESO, La Silla, in the period of July 2-11, 1995, using the MPIfR bolometer, operated at 230 GHz (1.3 mm, with a bandwidth of 50 GHz). The general properties of the bolometer are described in Kreysa (1990). The SEST telescope has a half power beam width (HPBW) of about $23''$. The total observing time scheduled was 84 hours, where we lost about 2.5 hours due strong wind, bolometer preparation and pointing tests.

The observations were done in a standard beam-switching method performing ON-OFF measurement of each source. An OFF position was achieved by moving the telescope slightly, about $70''$ in azimuth. The integration time at each ON and OFF position was 10 sec. Each observing scan consisted of 10 of such ON-OFF measurements, which gave on-target time of 100 s and off-target time of 100 s. We obtained 10 scans for each WR star observation. All but three of the WR stars (WR 90, WR 95, WR 113) were observed at least twice during the

TABLE 2.1— Spectral type, extinction and optical magnitude of the WR stars in this study, adopted from the compilation of van der Hucht (2001). The letter 'd' in the spectral type denotes WR stars which show excess infrared fluxes due to dust formation. Magnitudes *b* and *v* are in the system of Smith (1968).

No.	Star	Spectral type	A_v	*b*	*v*
			mag	mag	mag
1	WR 48	WC6 (+O9.5I)	0.93	5.76	5.88
2	WR 52	WC4	2.30	10.15	9.86
3	WR 63	WN7+OB	6.03	14.09	12.81
4	WR 65	WC9d+OB?	7.62	15.91	14.50
5	WR 78	WN7h	1.67	6.81	6.61
6	WR 79	WC7+O5-8	1.54	6.96	6.95
7	WR 81	WC9	6.36	13.81	12.71
8	WR 90	WC7	0.86	7.33	7.45
9	WR 95	WC9d	7.37	15.29	14.00
10	WR 105	WN9h	8.63	14.76	12.92
11	WR 111	WC5	1.05	8.21	8.23
12	WR 112	WC9d+OB?	12.24	20.10	18.80
13	WR 113	WC8d+O8-9IV	3.23	9.89	9.43
14	WR 48a	WC8ed+?	10.13	18.50	16.80

TABLE 2.2— 230-GHz flux densities of the programme WR stars and their *JHKL′M* magnitudes, quoted from van der Hucht, Williams, Setia Gunawan (in preparation).

Star	*J*	*H*	*K*	*L′*	*M*	230 GHz
	mag	mag	mag	mag	mag	mJy
λ_0 (micron)	1.24	1.63	2.19	3.78	4.66	1300
WR 48	5.56±0.06	5.53±0.06	5.43±0.07	5.34±0.05	5.26±0.07	12± 8
WR 52	8.48±0.03	8.21±0.05	7.59±0.12	7.36±0.07	6.84±0.18	23±11
WR 63	9.01	8.40	7.64	7.12		34± 8
WR 65	8.58±0.03	7.51±0.07	6.49±0.11	5.37±0.18	4.97±0.22	26± 8
WR 78	5.44± 0.3	5.24±0.01	5.00±0.01	4.53±0.03	4.38±0.09	28± 7
WR 79	6.00±0.02	5.89±0.02	5.50±0.01	5.16±0.02	4.92±0.14	25± 8
WR 81	8.32±0.03	7.76±0.04	7.15±0.02	6.53±0.04	6.05± 0.2	16± 5
WR 90	6.30±0.03	6.14±0.03	5.63±0.04	5.31±0.04	5.04±0.16	20± 6
WR 95	8.38±0.06	6.60±0.05	5.14±0.09	3.44±0.07	3.01±0.02	23±10
WR 105	7.07±0.03	6.32±0.01	5.78±0.04	5.08±0.06	4.84±0.10	40± 7
WR 111	7.34±0.03	7.16±0.03	6.61±0.04	6.39±0.07	6.01±0.37	22± 7
WR 112	8.8±0.11	6.42±0.10	4.27±0.09	1.26±0.14	0.37±0.09	21± 7
WR 113	7.04±0.03	6.26±0.06	5.38±0.09	4.29±0.14	3.96±0.09	16± 9
WR 48a Ft	8.44	6.85	5.02	2.88		55±11
WR 48a Br	6.74	4.18	2.16	0.03	–0.29	55±11

Note: Br= bright; Ft= faint

observing period.

For each observed source we performed a pointing observation, a sky dip (to measure the atmospheric transmission) and source observation (WR star or calibrator). Conversion to absolute flux density was done by using Mars and Uranus as calibrator. The flux densities of these planets during the observation were between 177.8 Jy (on July 02) to 164.4 Jy (on July 12) for Mars, and between 39.3 Jy (on July 02) to 39.5 Jy (on July 12) for Uranus. The flux density variation is due to the change of the planets geocentric distances as the planets move in their orbits.

The reduction (including the calibrator flux density calculation) was carried out using the standard continuum reduction package available at the SEST location. The data were corrected for airmass, atmospheric transmission and gain-elevation variation and then the scans were converted into flux-density units. The main source of uncertainty is the atmospheric transmission variation. The error due to bad pointing is typically about 10% (Whyborn, private comm.).

During the 1.3-mm observations we witnessed quite varying weather conditions: from fair, clear sky to some days with strong winds, high humidity, and even snow falls. This resulted in some data with high, variable sky noise. Some data for a star from consecutive nights show large variations, which we attribute to be due to the variable whether. Therefore, instead of averaging the data from consecutive nights, we choose those with the highest signal-to-noise ratio. In Tab. 2.2, we list 1.3-mm results only for 14 WR stars out of the 22 observed stars. Four of the listed star were not detected at the 3σ detection, and therefore, their 1.3-mm data were excluded from further analysis. We keep their data in the table as, will be shown later, at least for WR 48, the data seem to be in agreement with data at other wavelengths.

2.2.2 Near infrared data

The 1.3-mm data are combined with $JHKL'M$ magnitudes (see Tab. 2.2), which were collected in a monitoring program of WR stars, originally aimed at finding IR-variable WR stars. A full description of the observations is presented in a separate paper (van der Hucht, Williams, Setia Gunawan, in preparation), which also presents the complete data of the monitoring program. Below is a summary of the observations.

The IR photometry was obtained at the 1-m, 2.2-m and 3.6-m telescopes of the European Southern Observatory (ESO) on La Silla, Chile, the 3.8-m United Kingdom Infrared Telescope (UKIRT) on Mauna Kea, Hawaii, the 1.52-m Carlos Sanchez Telescope (CST) on Tenerife, Canary Islands, and at the 3.9-m Anglo-Australian Telescope. The $JHKL'M$ filters in use at the four observatories are essentially similar, and are listed on Tab. 2.2.

The IR photometry was obtained two to five times per epoch, in consecutive nights which was then averaged to present the data of that epoch. Typical uncertainties in $JHKL'$ magnitudes are ~ 0.03 mag, while the M magnitudes suffer from errors about twice as large. For the present study we further average these data, as presented in Tab 2.2, together with the standard deviation of the mean. In the infrared, WR 48a is known to show strong variability. Therefore, in Tab. 2.2 we separated its IR data: the maximum and the minimum magnitudes.

2.2.3 Analysis

We supplemented the NIR and sub-mm data with data from the MSX (Midcourse Space eXperiment) satellite and from the IRAS Point Source Catalogue (PSC). Radio data available

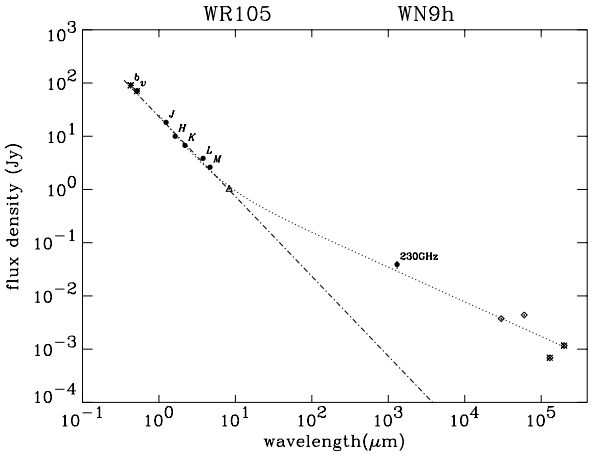

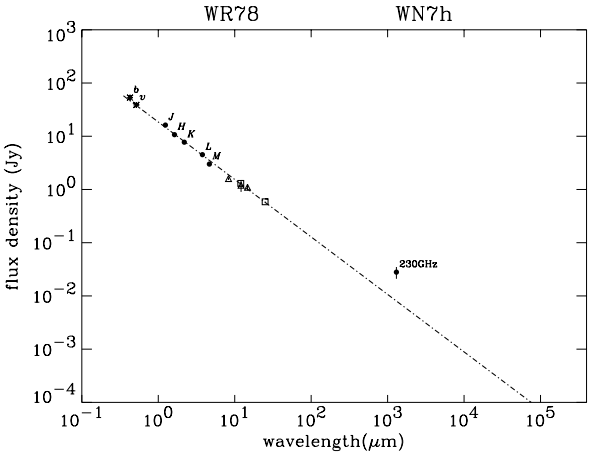

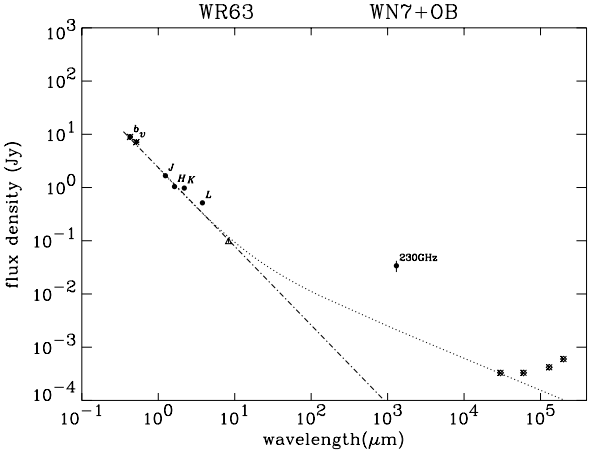

FIGURE 2.1— De-reddened flux-density of WN stars. The symbols are: (•) data obtained in this study, (∗) for the adopted *b* and *v* data, (△) for MSX data, (□) for IRAS data, (◇) for the radio data. The error bars for the *JHKL′M* are in most cases smaller than the • symbol. Upper-limit radio data are marked ⊠.

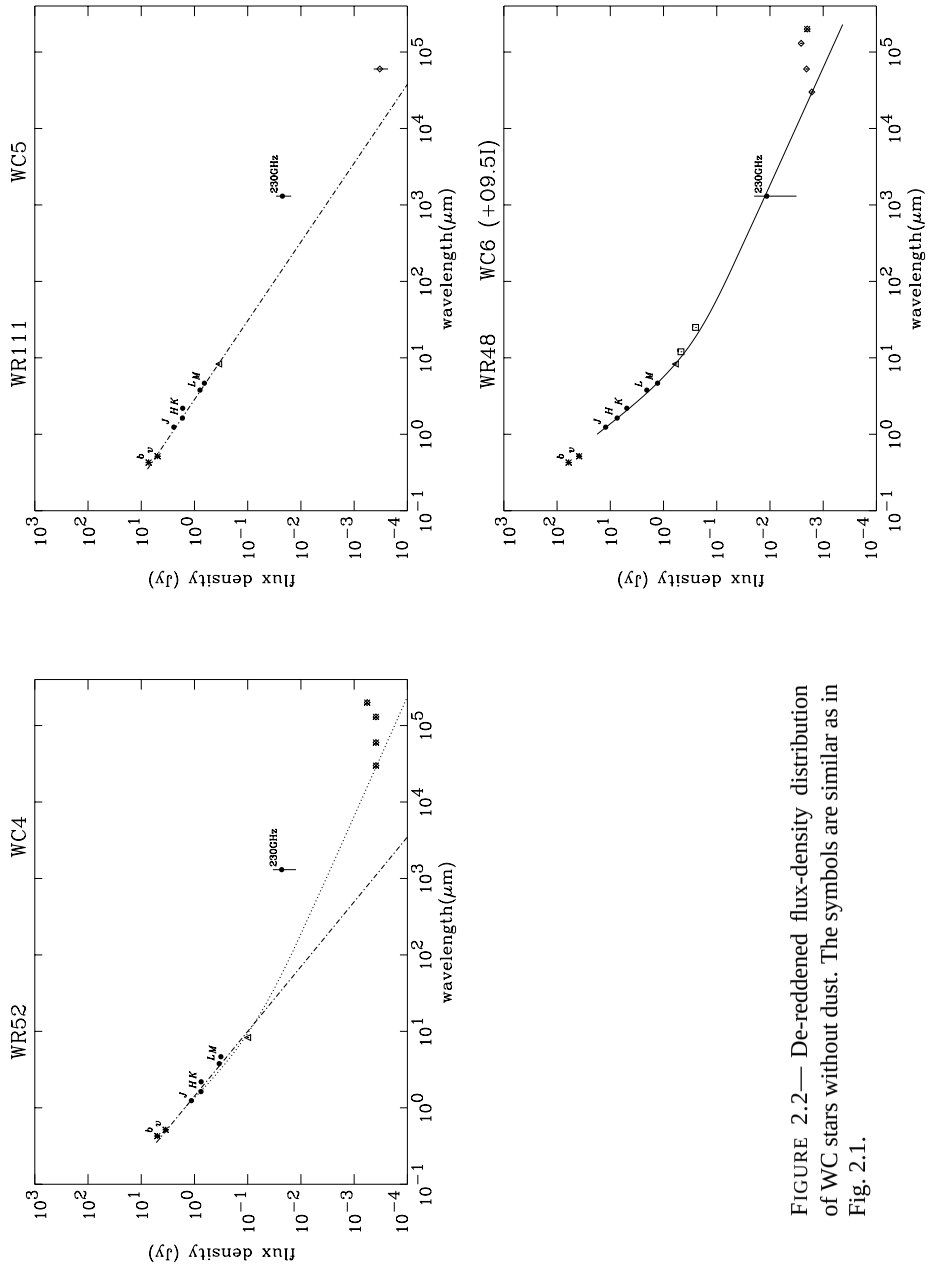

FIGURE 2.2— De-reddened flux-density distribution of WC stars without dust. The symbols are similar as in Fig. 2.1.

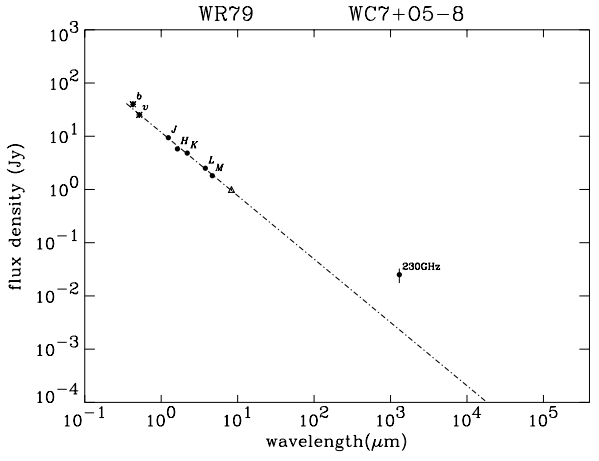

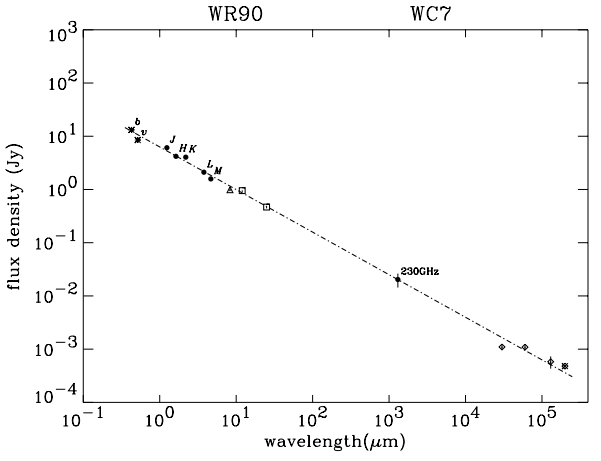

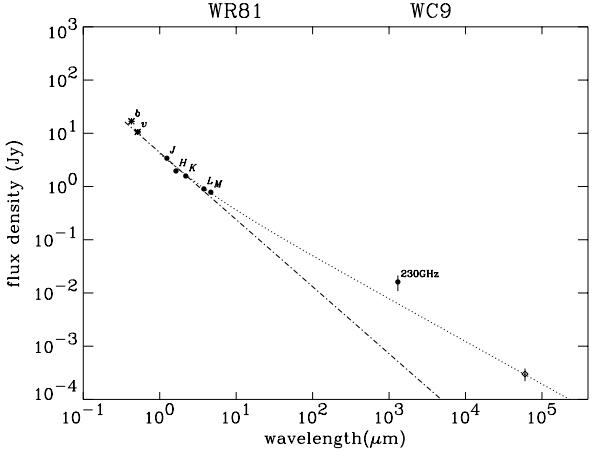

FIGURE 2.3— De-reddened flux-density distribution of WC stars without dust (continued).

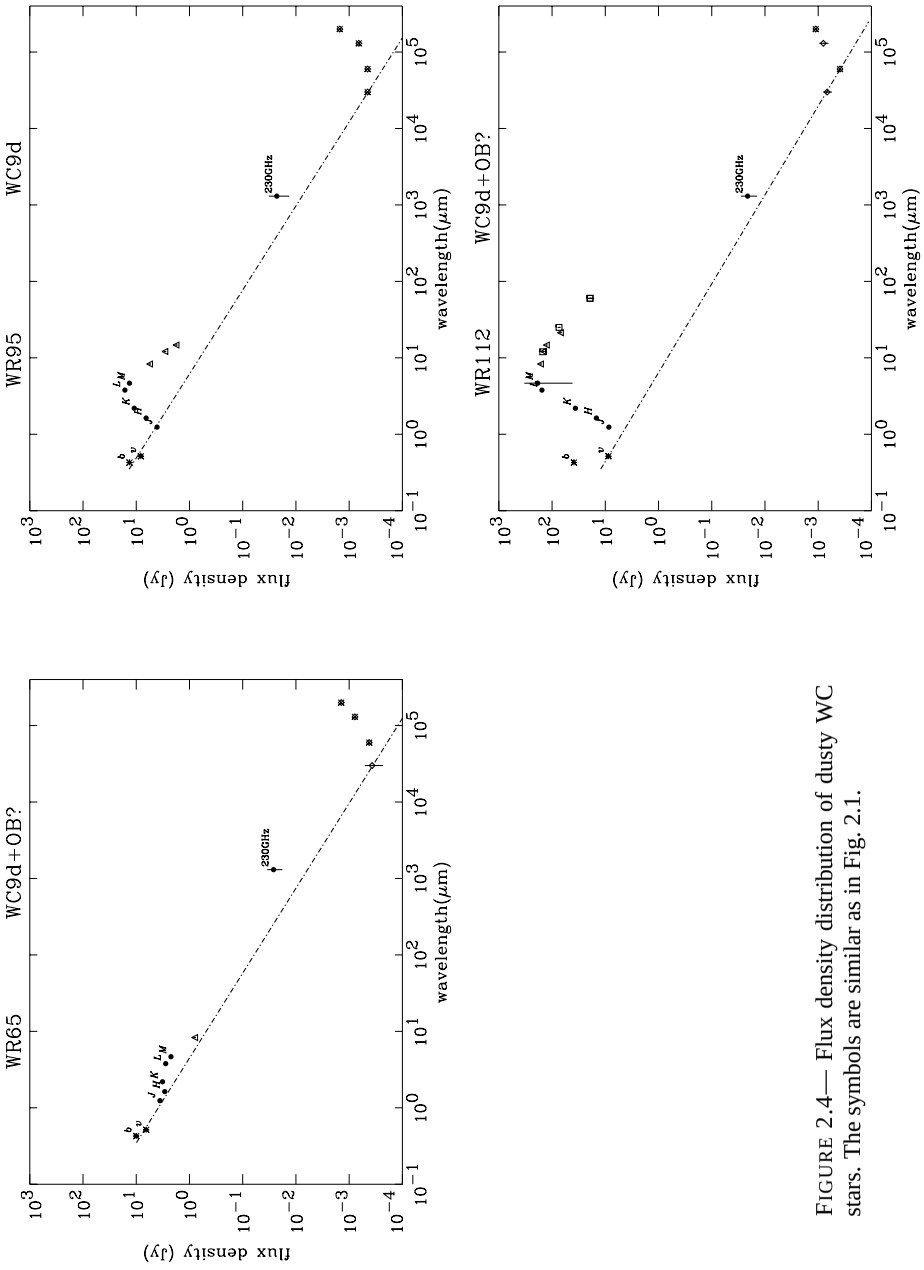

FIGURE 2.4— Flux density distribution of dusty WC stars. The symbols are similar as in Fig. 2.1.

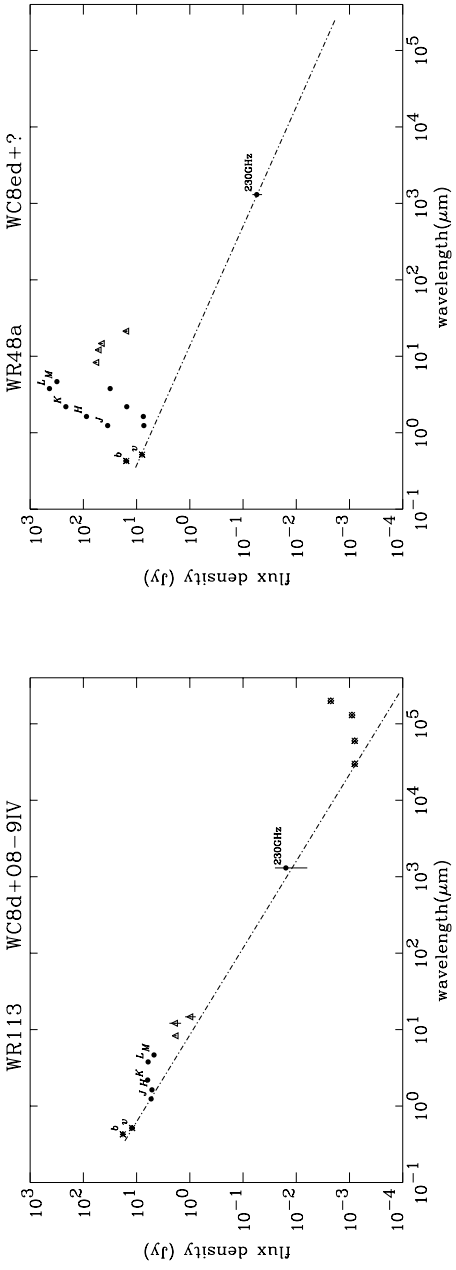

FIGURE 2.5— Flux-density distribution of dusty WC stars (continued)

TABLE 2.3— Spectral indices of the single power-law fit to the FDDs. The errors are the standard deviation of the data to the fit.

Non-dusty WR stars		α	σ	Remarks
WR 105	WN9h	1.50	0.04	Optical-NIR-MSX
WR 78	WN7h	1.08	0.04	All
WR 63	WN7+OB	1.48	0.04	Optical-NIR
WR 52	WC4	1.18	0.05	Optical-NIR
WR 111	WC5	0.97	0.02	NIR
WR 48	WC6 (+O9.5I)	1.46	0.06	Optical-NIR
WR 90	WC7	0.80	0.04	All
WR 79	WC7+O5-8	1.19	0.02	Optical-NIR-MSX
WR 81	WC9	1.26	0.04	Optical-NIR
Average		1.21	0.24	
Dusty WR stars				
WR 65	WC9d+OB?	0.90	0.02	Optical-3cm
WR 95	WC9d	0.91	0.02	Optical-3cm
WR 112	WC9d+OB?	0.86	0.02	*v*-3cm-6cm
WR 113	WC8d+O8-9IV	0.88	0.02	Optical-*J*-3cm
WR 48a Ft	WC8ed+?	0.64	–	*v*-230GHz
Average		0.84	0.11	
Overall Average		1.08	0.27	

for the stars in our study are mostly from Chapman et al. (1999) for WR 48, WR 52, WR 63, WR 65, WR 90, WR 95, WR 105, WR 112, WR 113, at 3, 6, 13, 20 cm. We also used results of Abbott et al. (1986) for WR 81 and Bieging et al. (1986) for WR111, both at 6 cm.

The optical and NIR data were de-reddened by adopting the interstellar extinction law of Rieke and Lebofsky (1985). The compiled data are shown in Figs. 2.1–2.5. We note that the data for the flux density distribution (from here on FDD) were taken at different epochs, which means that variability may be included in the figures. The different instruments used to obtain the data have different apertures: $\lesssim 15''$ for *JHKL′M*, $18\farcs3$ for MSX (resolution), $> 30''$ for IRAS (resolution), and $23''$ for 230-GHz (HPBW) data. The radio data have an angular resolution of $\leq 12''$. Therefore, FDD may also be contaminated by extra emission falling on the larger apertures.

We found that the FDDs of WR 78 and WR 90 can be represented by a power law spectrum with single index, $S_\nu \propto \nu^\alpha$. Linear fits (using a least absolute deviation method) in the $\log S - \log \nu$ space of these two stars give spectral indices α(WR 78) = 1.08 and α(WR 90) = 0.79. The optical to NIR data of WR 52, WR 79, WR 81, WR 105 and WR 111 can also be fitted with a single-index power-law spectrum: α(WR 52) = 1.18, α(WR 79) = 1.18, α(WR 81) = 1.26, and α(WR 111) = 1.01. The standard deviations of the fits are between 0.02–0.05. Single power-law fits to the optical-NIR data of WR 48, WR 63 and WR 105 give high values: α(WR 48) = 1.46, α(WR 63) = 1.48, and α(WR 105) = 1.50. The average of these spectral indices is $< \alpha > = 1.21$ ($1\sigma = 0.24$). The spectral indices are shown in Tab. 2.3.

We observe that there are significant differences in spectral trends between some stars at

around mid-IR (WR 48, WR 52, WR 63, WR 105). This trend difference is clearly visible in the radio fluxes which fall high above the single power-law spectra. We found that in the case of WR 48 a double power-law spectrum of the form:

$$S_\nu = C_1\nu^{\alpha_1} + C_2\nu^{\alpha_2}, \tag{2.1}$$

where C_1 and C_2 are coefficients, can be drawn through the infrared points down to the highest radio frequency.

The dusty WR stars require more detailed fitting which should include the IR excess emission due to dust, which is beyond the present study. Therefore, for these stars, we fit a single power law to the least enhanced NIR points and the highest radio frequency points. The spectral indices are shown in Figs. 2.1–2.5.

2.3 Discussion

The spectral indices of the non-dusty stars (excluding that of WR 48), were obtained taking mainly the optical and NIR data into consideration. Therefore, we can compare this with the results of Morris et al. (1993). We can not find any differences between the WC and the WN stars, nor any trends in spectral types. The average of the spectral indices of 1.21 ± 0.24 in our sample is significantly higher than 0.85 ± 0.26 obtained by Morris et al. (1993). However, we note that our sample is smaller and does not cover the all WR spectral subtypes, to be able to draw such conclusions.

Below we give notes to each star, separated into non-dusty WR stars and dusty ones.

2.3.1 Non-dusty WR stars

WR 105 (WN9h). The 230-GHz and radio flux densities are much higher than the value expected form the single power-law fit. We suggest that there is a change of spectral index trend in this star. A double power-law spectrum as in WR 48 may be applicable for this star. In Fig. 2.1, we also plotted a spectra for $\alpha_1 = 1.94$ and $\alpha_2 = 0.65$.

WR 78 (WN7h). The optical to IRAS data of this star can be fitted with a single power-law. This makes the 230-GHz flux density higher than expected from the fit. However, we have no radio observation from this star to further constrain the fit. From the single power-law fit result, the radio flux density is expected to be very faint. However, there is a chance that this star shows also the trend change. In which case, if we assume that the 230-GHz data is correct, we can expect it show to show significant radio emission, observable by the Australia Telescope Compact Array (ATCA). We can also change the argument around, where we use the radio result to confirm whether this star show a change of trend in spectral index or not.

WR 63 (WN7+OB). The single power law fitted to the optical to NIR data is rather steep, making the upper limit radio flux density of Chapman et al. (1999) to be much brighter than expected from the fit. The 230-GHz data is much too high. However, we could not find any source nearby that may have been observed within the SEST HPBW. This may be a result of either the bad calibration or a change in weather condition or a previously unobserved source in the beam.

WR 52 (WC4). At first instance this star may seem to have an infrared excess. However, Williams & Allen (1980) showed that the 2-micron spectrum of WR 52 is dominated by the 2.06 μm HeI emission line. This line dominates the *K*-band flux, while the *H*-band flux is dominated by strong CIV lines. After correction for the emission lines, Williams & Allen

(1980) showed that WR 52 is just an ordinary WC4 star without any IR excess. The 230-GHz flux density is much higher than the fit, and we cannot find another source nearby that may fall into the SEST aperture.
The radio flux densities are brighter than the value expected from the single power-law fit, showing a change in the spectral index at around mid-IR.

WR 111 (WC5). The optical to NIR spectra can be represented by a single power law. The 230-GHz flux density is much higher than the fit, and we cannot find another source nearby that may fall into the SEST aperture. The radio flux density is also higher than the fit. There are several reason that can be used to explain this. Either the radio data result from a non-thermal emission or the star has a change in the spectral index, or a combination of both.

WR 48 (WC6+(09.5I)). The single power-law fit to the data of this star gives a steep spectrum. However, we can draw a double power-law spectrum through the data points. This system shows non-thermal phenomena at radio frequencies, which make it very interesting as this star is known to be a binary with period of only 18 days. Non-thermal emission in binary systems is thought to originate in between the binary components, where the winds of the two stars collide. For this 18-d period binary the interaction region will still be inside the radiophotosphere. One solution for the non-thermal radio emission to overcome the free-free absorption from the radiophotosphere is that the binary is actually a triple-star system, as first suggested by Moffat & Seggewiss (1977), where the third component is further away. In this way, the non-thermal radio emission should originate from between the third star and the close binary.

WR 79 (WC7+O5-8). This star shows similar proportions as WR 78 (WN7h): we have no radio data to constrain the fit and the fit of the optical to NIR data points puts the 230-GHz data high above the fit. However if this star also shows a change of spectral trend, then we may have a correct 230-GHz flux density. Radio data of this star, where ATCA is well suited to obtain them, are clearly needed to establish whether there is a change of spectral trend involved or whether a single power law fit is sufficient to describe the spectra of this star.

WR 90 (WC7). The FDD can be fitted nicely by a single power law. The radio data show a clear thermal spectrum. The fitted spectral index of $\alpha = 0.8$ is higher than $\alpha = 0.6$ expected from a spherically symmetric, steady state wind. This make this single, non-dusty star interesting to be observed into more detail, so that we can have an insight into the wind structure and how it deviates from the conditions in the model of Wright & Barlow (1975).

WR 81 (WC9). The 230 GHz and radio data for this star are higher than the value expected from the fit of the optical to IR data. However, a double power law may also applicable to this star.

2.3.2 Dusty WR stars

The dusty WR stars are characterised by strong infrared excesses, which makes it difficult to find the wind spectra of these stars. For those having radio data, the spectral indices were obtained from the 3-cm data and the *J*-band fluxes, showing that the 230-GHz data are in all cases higher than the fit flux density. This may be due to the dust contributing to the 230-GHz flux density, or, there may be variability in the radio flux density. We noted that all radio data show negative spectral indices, characteristic of non-thermal emission. In all but one case (WR 95), the objects are binary systems. A high resolution infrared image may reveal whether WR 95 is truly a single star or a binary.

WR 113 (WC8d+O8-9IV). The 12.6 micron MSX data may be contaminated. The radio data may point to non-thermal phenomena. We note that this is a 30-d period binary and the wind-collision zone may be buried within the radiophotosphere. If the non-thermal phenomena are a result of colliding winds, then this star may be another triple-star system.
WR 48a (WC8ed+?). This star shows occasions when it is much brighter than at other times. This is associated with periods of more active dust formation. The MSX data are consistent with the NIR data at the faint epochs. If the *J* to 230-GHz fit is true, then this star should be observable at radio frequencies. Otherwise, we may still observe a dust contribution at 230 GHz.

2.4 Summary

We summarize as follow:
1. The NIR data points can, in most cases be fitted by single power-law spectra.
2. The average spectral index is $< \alpha > = 1.21$ ($1\sigma = 0.24$) for non-dusty WR stars and $< \alpha > = 0.84$ ($1\sigma = 0.11$) for dusty WR stars. The overall average is $< \alpha > = 1.08$ ($1\sigma = 0.27$).
3. We confirm, with our limited sample, the result of Morris et al. (1993), that the spectral index shows no dependency on spectral type.
4. A change of trends of the spectral index at around mid-IR is observed in some stars, where the spectral indices are shallow, close to the theoretical value of $\alpha = 0.6$ at long wavelengths, and become steeper towards NIR-optical wavelengths, closer to $\alpha = 2$ of the Rayleigh-Jeans tail.
5. The binaries in the non-dusty group show spectral indices which are higher than those of the known single WR stars. However, WR 105 (WN9h), so far known as single star, shows also a steep spectral index.